Journal of Hydrology 639 (2024) 131612

Contents lists available at ScienceDirect

Journal of Hydrology

journal homepage: www.elsevier.com/locate/jhydrol

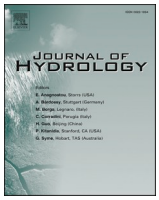

Research papers

Hydrologic responses to wildfires in western Oregon, USA

Hyunwoo Kang [a,*], Ryan P. Cole [a], Lorrayne Miralha [b], Jana E. Compton [c], Kevin D. Bladon [a,d]

[a] Department of Forest Engineering, Resources, and Management, Oregon State University, Corvallis, OR, USA
[b] Department of Food, Agricultural and Biological Engineering, Ohio State University, Columbus, OH, USA
[c] U.S. EPA, Office of Research and Development, Center for Public Health and Environmental Assessment, Pacific Ecological Systems Division, Corvallis, OR, USA
[d] Department of Forest Ecosystems and Society, Oregon State University, Corvallis, OR, USA

ARTICLE INFO

This manuscript was handled by Sally Elizabeth Thompson, Editor-in-Chief, with the assistance of sally Elizabeth Thompson Gerlein-Safdi, Associate Editor

Keywords:
Budyko curve
Potential evapotranspiration
Random Forest
Streamflow
Wildfire

ABSTRACT

Wildfires can dramatically alter vegetation cover and soil properties across large scales, resulting in substantial shifts in runoff generation, streamflow, and water quality. In September 2020, extensive and high-severity wildfires burned more than 490,000 ha of forest land on the westside of the Cascade Mountain Range in the Pacific Northwest. Much of the area impacted by these fires is critical for the provision of water for downstream aquatic ecosystems, agriculture, hydropower, recreation, and municipal drinking water. We undertook a study to evaluate the effects of four of the large high severity wildfires from 2020 (Riverside, Beachie Creek, Lionshead, and Holiday Farm) on streamflow in nine burned catchments in western Oregon. We also included four unburned, reference catchments in our analysis to enable us to assess post-fire streamflow changes in the burned catchments. To quantify the effects of wildfire on the catchment water balance we used publicly available streamflow data and estimated precipitation, potential evapotranspiration (PET), and actual evapotranspiration (ET), using satellite-based meteorological data. We quantified catchment area burned and burn severity with the average differenced normalized burn ratio (dNBR). We compared hydrologic conditions for the pre-fire (2001–2020) and post-fire (2021–2022) periods by analyzing catchment runoff ratios, ET ratios (evaporative index: quotient of ET divided by precipitation, referred to as EI hereafter), and Budyko curves. We also used random forest models to explore factors influencing the variability in EI. During the post-fire period, we observed decreases in EI and increases in runoff ratio in the burned catchments. Post-fire declines in EI were positively related to burn severity ($R^2 = 0.70$ in 2021; 0.76 in 2022) and area burned ($R^2 = 0.91$ in 2021; 0.95 in 2022), and were primarily driven by decreases in ET. Declines in ET were highly variable, ranging from 10.7–40.2 % in the first year after the fires and 6.1–32.0 % in the second year after the fires, and were generally related to catchment burn severity and area burned. The greatest increases in runoff (16.1 % in 2021 and 19.8 % in 2022) occurred in the same catchment. These results were reinforced by the random forest analysis, which illustrated the importance of burn severity as a predictor of EI. Interestingly, the variability in changes in EI during the post-fire period was also associated with other geomorphic factors such as catchment slope, elevation, geology, aspect, and pre-fire vegetation type. Since the duration and seasonality of post-fire impacts on hydrology remain uncertain, our findings bring new insights and guide future studies into the post-fire responses on hydrology that are crucial for water and forest management.

1. Introduction

In recent decades in many regions of the world, including the western United States, there have been substantial shifts in wildfire regimes, including longer wildfire seasons, increased area burned, and greater wildfire severity (Abatzoglou and Williams, 2016; Burke et al., 2021; Holden et al., 2018; Westerling, 2016). Fire, as a natural disturbance, is a fundamental component of global ecosystems, burning vast areas (~300–450 Mha) each year (van der Werf et al., 2006). However, the increasing occurrence of large, high severity wildfires has been linked with periods of extreme heat and increasing occurrence of drought conditions (Abatzoglou et al., 2019, 2017; Jolly et al., 2015). Across the western United States, climate change has contributed to an additional 4.2-million ha of forest area burned between 1984 and 2015 (Abatzoglou and Williams, 2016). Rapid and substantial shifts in the wildfire regime have increased concerns about the longer-term impacts on

* Corresponding author.
E-mail address: hyunwoo.kang@oregonstate.edu (H. Kang).

https://doi.org/10.1016/j.jhydrol.2024.131612
Received 20 March 2024; Received in revised form 29 May 2024; Accepted 19 June 2024
Available online 2 July 2024

biophysical systems and humans, leading to calls for more integrative and predictive research to enable mitigation or adaptation efforts (Shuman et al., 2022).

Forests are a crucial source of a reliable water supply to communities around the globe (Dudley and Stolton, 2003), providing the majority of freshwater in many regions, including the United States (Jones et al., 2009). Healthy forests provide substantial social and economic benefits through provision of a high-quality water supply (Bladon et al., 2014; Costanza et al., 1997). However, the recent shifts in wildfire regime and growing pressures on water supplies have increased concerns regarding the impact of wildfires on water supplies (Hallema et al., 2018a; Hohner et al., 2019). As a result, research has increased in recent years, illustrating wildfire effects on water quantity and water quality, including suspended sediment, nutrients, carbon, and heavy metals (Beyene et al., 2023; Rhoades et al., 2019; Rust et al., 2018). Wildfires can also affect soil hydraulic properties or increase soil water repellency, leading to reduced infiltration rates (Moody et al., 2015; Moody and Ebel, 2014; Neary, 2011; Thomas Ambadan et al., 2020), and elevated surface runoff, erosion, and suspended turbidity (Chen et al., 2020; Ebel et al., 2012). Many of these effects pose substantial challenges for drinking water treatment and can impact aquatic ecosystem health (Emelko et al., 2016, 2011; Hohner et al., 2019; Warren et al., 2022).

In recent years, there has also been an increase in the number of studies quantifying the effects of wildfires on initial and longer-term shifts in hydrological processes (Niemeyer et al., 2020; Poon and Kinoshita, 2018). These studies have generally illustrated an increase in net precipitation and soil water content due to fire-related decreases in interception storage capacity and evapotranspiration from reductions in canopy vegetation or ground cover (Zema, 2021). A recent assessment of approximately 5,500 wildfires across the contiguous United States illustrated substantial post-fire decreases in ET, especially in the western United States (Collar et al., 2021). Similarly, Ma et al. (2020) quantified a 23–36 % reduction in annual evapotranspiration during the first 15 years after wildfires in California's Sierra Nevada, while Poon and Kinoshita (2018) observed 11–36 % lower ET in burned catchments compared to unburned catchments following the 2011 Las Conchas Fire in New Mexico.

Wildfire impacts on hydrologic processes can also lead to elevated runoff generation (Boisramé et al., 2019; Hallema et al., 2018b; Vieira et al., 2018; Zituni et al., 2019), increased peak flows, low flows, annual water yields, and shifts in the timing of the hydrograph (Beyene et al., 2021; Lavabre et al., 1993; Robinne et al., 2020; Williams et al., 2022). However, there remains substantial uncertainty about the post-fire streamflow response. For example, in a study of 168 locations across the U.S., regional streamflow in the first five years after wildfire ranged from a decrease of 37.1 % to an increase up to 27.4 % (Hallema et al., 2018b). Similarly, many other studies of wildfire effects on annual water yields in different regions and catchment areas have observed no effect up to a 450 % increase (Bart, 2016; Niemeyer et al., 2020; Wine and Cadol, 2016). In western North America, others have also observed post-fire increases in peak flows of 20–290 % (Brogan et al., 2017; Mahat et al., 2016) and increases in low flows of 40–1,090 % (Kinoshita and Hogue, 2015; Saxe et al., 2018). The variability in post-fire streamflow responses has been attributed to site-specific factors including, but not limited to, burn severity, percent area burned, post-fire precipitation, catchment slope, aspect, and aridity (Moody et al., 2013; Noske et al., 2016; Rhoades et al., 2011; Wampler et al., 2023). As such, there remains a need to continue to improve our understanding of the complex interplay between wildfire, catchment physiographic characteristics, and the streamflow response.

Due to drought conditions, low fuel moisture, low relative humidity and high winds, the 2020 Labor Day Fires consisted of five simultaneous mega-fires that ultimately burned more than 4,900 km^2 of forest land in the Oregon Cascades, United States. The occurrence of these 2020 wildfires allowed us to compare multiple simultaneous large, high severity wildfires across catchments with variation in physiography. As such, our objectives were to (a) quantify and compare the effects of these wildfires on the hydrologic response across nine burned catchments in western Oregon, and (b) relate the responses to burn severity, catchment area burned, and catchment physiographic characteristics, such as elevation, slope, geology, aspect, and vegetation type. To achieve our objectives, we applied the Budyko method (Budyko, 1961; Budyko, 1974; Wang and Hejazi, 2011) to characterize the competition between energy and water availability in our study catchments. We then used the Budyko curves to characterize and assess the hydrologic responses in burned catchments and compared those with unburned catchments over the same time period. We also applied random forest models to demonstrate the potential wildfire or catchment controls on the hydrologic response.

2. Methods

2.1. Study catchments

Our study basins were located in the western Cascade montane highlands and lowlands of the Willamette River basin in Oregon. The region is characterized by a Mediterranean climate with warm and dry summers and wet winters (Kottek et al., 2006). The annual average precipitation varies from 1,000 to 3,000 mm due to orographic effects. In the lower elevation areas (<200 m), annual 30-year normal temperatures range from minimums of 1.0–10.7 °C in the winter to maximums of 9.0–27.6 °C in the summer. In the high elevation areas (>1,800 m) temperatures range from minimums of −8.5–2.7 °C in the winter to maximums of −1.1–22.2 °C in the summer (PRISM Climate Group, 2022). The region is dominated by forested lands primarily composed of Douglas-fir (*Pseudotsuga menziesii*) and mountain hemlock (*Tsuga mertensiana*) tree species (Busing, 2004). This region is mostly composed of volcanic and surficial sediments lithology (Madin, 2009).

In the summer of 2020, a series of large and high-severity wildfires burned approximately 494,000 ha in western Oregon, which was the second largest wildfire season on record in the region (Rasmussen et al., 2021). The rapid spread of these fires was facilitated by strong downslope east winds and prolonged warm and dry conditions, which persisted for over 60 days (Abatzoglou et al., 2021; Higuera and Abatzoglou, 2021). Our study focused on 13 catchments in the Cascade Range of Oregon, including nine burned (B1 to B9) and four unburned (U1 to U4) catchments (Fig. 1). Our study area included catchments that were affected by four wildfires—the Riverside, Beachie Creek, Lionshead, and Holiday Farm fires—which burned a combined area of ~ 284,971 ha. Across the four wildfires, 37.1 % of the area burned at high severity, 23.8 % burned at moderate severity, 30.0 % burned at low severity, while 9.1 % remained unburned (Table S1). These fires burned in the Sandy, Clackamas, South Santiam, North Santiam, and McKenzie River Basins, all draining into the western side of the Willamette River Basin. Within the 13 burned and unburned catchments in our study area, there were 124 Hydrologic Unit Code 12 (HUC12) sub-watersheds.

Across the 13 study catchments, the long-term (2001–2020) average annual precipitation ranged from 1,793 mm to 2,453 mm with strong orographic effects associated with the Cascade Mountains (Fig. 2). The long-term average annual air temperature ranged from 7.1 °C to 10.0 °C (Abatzoglou, 2013). The burned catchments had a range in burn areas, burn severities, and hydrogeologic characteristics, which provide a unique opportunity to compare the hydrologic response of wildfires in multiple catchments (Table 1).

2.2. Data

All burned and unburned catchments were delineated with the ArcHydro extension to ArcGIS 10.5 using the locations where long-term streamflow data were available (Table 1). To evaluate the hydrologic response to wildfire disturbances, we assembled data layers for precipitation, actual ET (AET), potential ET (PET), and streamflow for the pre-

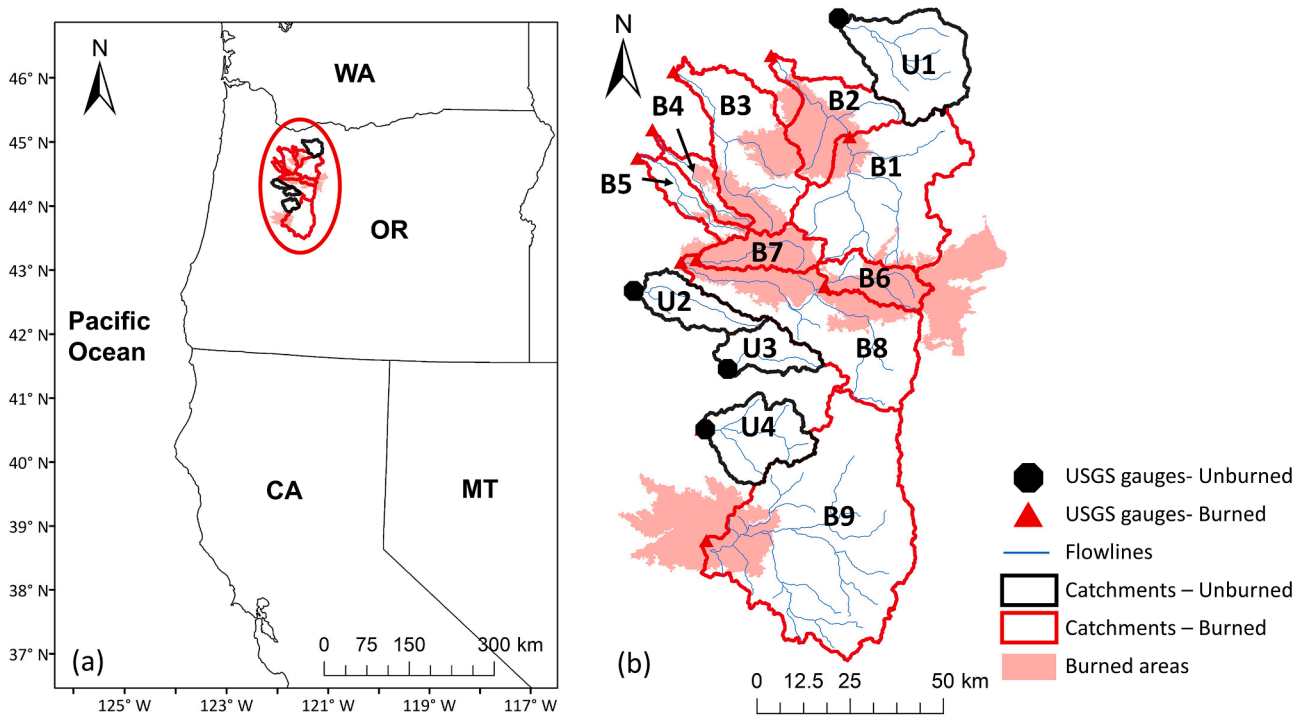

Fig. 1. (a) Map showing the location of our study sites (red circle) in the western United States. (b) Map of the study catchments. Red and transparent polygons represent the burned areas of the four wildfires burned in 2020 (from north to south: Riverside, Beachie Creek, Lionshead, and Holiday Farm). Red and black lines indicate the boundary lines of burned and unburned catchments, respectively (B: Burned, U: Unburned). Also, red triangles indicate the USGS gauging stations for the burned catchment, and the black circles represent the unburned catchments.

fire (2001–2020) and post-fire (2021–2022) periods. Precipitation and PET data were derived from a high-resolution (4 km) gridded dataset of surface meteorological variables (gridMET; Abatzoglou, 2013), and a total of 572 pixels were available for burned and unburned catchments. We grouped annual precipitation into dry years (9 to 11 years average; Fig. 2b) and wet years (9 to 11 years average; Fig. 2c) by comparing the annual precipitation with the long-term mean annual precipitation (2001–2020). The spatial pattern of precipitation during the first post-fire year (2021; Fig. 2d) was visually similar to the dry years, while the precipitation in the second post-fire year (2022; Fig. 2e) was similar to the wet years. In addition, remote sensing-based ET data from the Operational Simplified Surface Energy Balance (SSEBop; Senay et al., 2013) was applied to calculate the ET ratio and was used in the Budyko curve analyses. The SSEBop data was highly correlated with observed ET, and it has been used for some studies of post-fire hydrology (Blount et al., 2020; Collar et al., 2021; Poon and Kinoshita, 2018). However, since the SSEBop data is particularly sensitive to land surface temperature as an input (Chen et al., 2016) due to reduced albedo and the resultant rise in remotely sensed land surface temperatures within burned forests (Rother and De Sales, 2021; Rother et al., 2022), the ET estimates may exhibit uncertainties in areas burned at moderate to high severities. Additionally, further uncertainties could stem from the lack of proper validation of the SSEBop data with ground observations in the forests of the Pacific Northwest. Despite these uncertainties, the SSEBop data was utilized in this study because it provided long-term (2000 to 2022) and high-resolution (1 km) ET estimates. Furthermore, its reliability has been extensively validated across various regions of the United States (Collar et al., 2021; Poon and Kinoshita, 2018). The burned perimeters and burn severity data were provided by the Monitoring Trends in Burn Severity (MTBS; https://www.mtbs.gov) website. The burn severities were defined by the differenced Normalized Burn Ratio (dNBR; Key and Benson, 2006). For the burned catchments, the area burned ranged from 10.4 % to 94.2 %. The mean dNBR ranged from 53.5 to 565.1 with larger values of dNBR representing greater burn severity.

2.3. Analysis of hydrologic responses

The Budyko curve is an approach that enables exploration of the interactions between climate, vegetation, and catchment water yield (Budyko, 1974, 1961). The curve is based on the relationship between catchment PET and AET with both parameters normalized by precipitation. Previous studies have used the Budyko framework to assess the impacts of climate shifts and landscape disturbances on catchment hydrology and streamflow (Guo et al., 2021; Hampton and Basu, 2022; Jaramillo et al., 2018; Lee, 2020; Li et al., 2018; Wang and Hejazi, 2011; Wang and Stephenson, 2018).

We provide a conceptual diagram to summarize the principle of the Budyko curve method in Fig. S1. On the x-axis is the dryness index (DI), which characterizes the drying power of the atmosphere and the supply of water in the catchment, calculated as the ratio of PET to precipitation. A DI value greater than one indicates a dry, water-limited catchment, whereas a DI value less than one indicates a humid, energy-limited catchment (Fig. S1a). Comparatively, the evaporative index (EI) provides information about the potential water deficit or surplus in a catchment and is calculated as the ratio of AET to precipitation. A greater EI value indicates a larger proportion of precipitation that is involved in ET, resulting in less water available for streamflow. The Budyko curve can be developed for catchments to assess the degree to which disturbances, such as wildfire, result in deviations in the relationships between ET and precipitation, which would be indicative of shifts in water partitioning. Moreover, Budyko curves may be used to characterize catchment recovery in the water balance.

In our study, we applied the Budyko curve to nine catchments in western Oregon impacted by the 2020 Labor Day fires and four unburned, reference catchments. We fit our data to linear models rather than the non-linear parametric models, which are typically used to model data in Budyko space. The parametric models are defined by

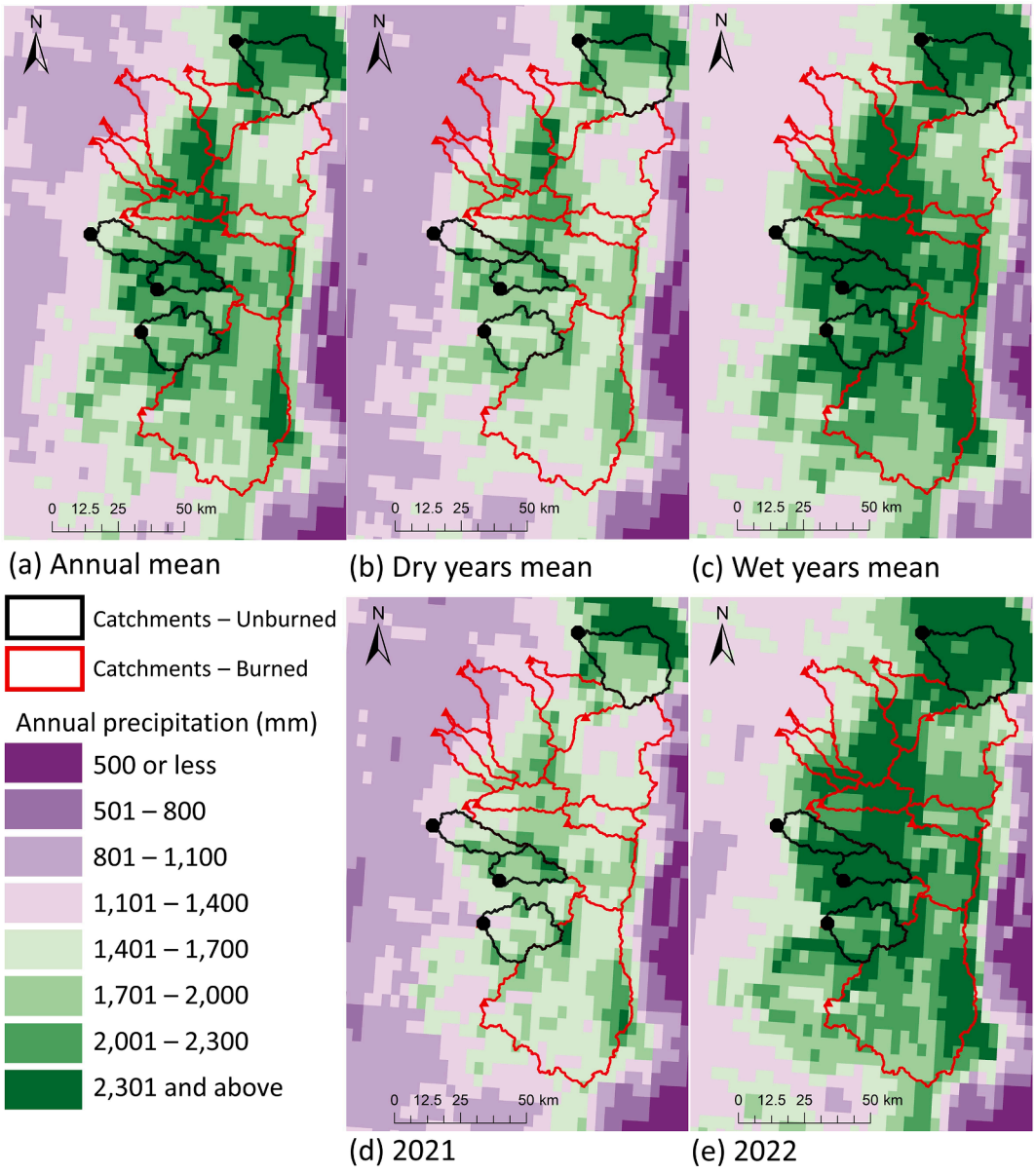

Fig. 2. Maps of the (a) long-term (2001–2020) mean annual precipitation, (b) dry years mean annual precipitation, (c) wet years mean annual precipitation, (d) 2021 (first year post-fire) annual precipitation, and (e) 2022 (second year post-fire) annual precipitation. The 13 catchment boundaries are shown on the maps with red lines indicating the burned catchments and black lines indicating the unburned catchments.

various non-linear equations to enforce structure on the Budyko model that incorporates physical assumptions about catchment hydrology, namely that the y-axis (EI) should asymptotically approach 1 (the water limit), and that catchment EI is more sensitive to changes in precipitation for lower values of DI (x-axis), but is energy limited at this range (Reaver et al. 2022). However, the mathematical formulation of these parametric models is arbitrary and does not preclude the use of other methods to fit data in Budyko space (Reaver et al. 2022). Thus, while not the most common approach, the use of linear models are acceptable since our data does not approach the energy- or water-limited boundaries of the parametric Budyko models, and the DI in the post-fire years was within the range of pre-fire data. Additionally, our models reasonably meet the assumptions of linear regression regarding independence, normality of residuals, and homoscedasticity of variances.

To assess the post-fire impacts on catchment water partitioning, we quantified the changes in EI as the vertical Budyko deviation (Δd). This approach assumes that in the absence of a substantial catchment disturbance, such as wildfire, that the annual DI and EI will plot along a Budyko-type curve. Disturbances will result in deviation from the curve. As such, we calculated Δd as the difference between the fitted and measured EIs (Equation 1).

$$\Delta d = EI_f - EI_m \quad (1)$$

where EI_f is the fitted EI, and EI_m is the measured EI. More detailed descriptions of the use of the Budyko deviation approach are available from Hampton and Basu (2022).

We adopted an approach that involved using the vertical deviation (Δd) from linear models fitted in Budyko space to estimate the post-fire changes in EI. This approach enabled us to observe the pre-fire variability in Δd and establish confidence intervals around pre-fire EI expected values. Although our approach did not directly provide a *p-value* that quantified evidence of whether the post-fire years were from a different distribution, we calculated the probability of a standardized (internally studentized) residual occurring under the null hypothesis that the post-fire points were from the same distribution as the pre-fire data. To further test our hypothesis that wildfire significantly affected EI

Table 1
General descriptions of the burned and unburned watersheds (USGS: United States Geological Survey).

Catchment Numbers	Basin	USGS ID	Mean elevation (m)	Area (km^2)	Annual precipitation (mm; October to September)	Percent watershed area burned (%)	Mean dNBR
B1	Clackamas	14,209,500	1,077	1266.3	1,734	11.1	53.5
B2	Clackamas	14,210,000	852	1766.6	1,817	23.3	293.0
B3	Molalla-Pudding	14,200,000	590	845.7	1,843	36.5	142.9
B4	Molalla-Pudding	14,201,500	537	150.3	1,794	36.8	113.0
B5	Molalla-Pudding	14,200,700	514	188.9	1,619	15.7	40.8
B6	North Santiam	14,179,000	1,151	273.6	1,924	79.7	366.0
B7	North Santiam	14,182,500	822	285.2	2,185	94.2	565.1
B8	North Santiam	14,183,000	1,019	1691.8	2,072	52.8	135.9
B9	McKenzie	14,162,500	1,170	2409.4	1,937	10.4	52.7
UB1	Sandy	14,137,000	1,004	259.1	2,211	0.00	0.0
UB2	South Santiam	14,188,800	566	280.3	2,003	0.00	0.0
UB3	South Santiam	14,185,900	918	679.5	2,386	0.00	0.0
UB4	South Santiam	14,185,000	897	450.1	2,042	0.00	0.0

and Budyko relationships, we fit linear models to post-fire Δd values against catchment burned area and burn severity for all post-fire years.

Runoff and ET account for the loss of moisture from catchments and are sensitive to wildfire disturbances (Bart, 2016; Poon and Kinoshita, 2018). Thus, the overall hydrologic response to wildfires can be measured by comparing pre-and post-fire runoff and EI (Poon and Kinoshita, 2018; Saxe et al., 2018), with the magnitudes of difference deviating depending on the burn severity and catchment area burned (Wang et al., 2020). Therefore, we also calculated the annual runoff ratio for each catchment as the ratio of annual runoff (streamflow) to annual precipitation during each water year (October to September). To calculate the annual runoff ratio, we used observed streamflow from the USGS stations (Table 1) and gridMet precipitation.

Both runoff ratio and EI during the first post-fire year (2021) were compared with the average of dry years for the pre-fire period (2001–2020). We also compared runoff ratios and EI during the second post-fire year (2022) with the average of the pre-fire wet years. In addition, we computed bootstrapped 95 % confidence intervals for the change in runoff ratios for 2021 compared to pre-fire dry years (less than mean precipitation) and 2022 compared to the pre-fire wet years (defined as having greater than mean precipitation). We then fit linear models to the change in runoff ratios vs. burned area and burn severity for the wet and dry post-fire years.

2.4. Analysis of predictor variables of hydrologic response

We ran random forest models for both the pre-fire and post-fire periods to explore the strength of relationships between EI and catchment physiographic characteristics. Random forests are an ensemble machine learning technique that aggregates predictions from many decision trees and are useful for modeling non-linear relationships and interactions among predictor variables (Breiman, 2001). In our analysis, we were primarily interested in using variable importance outputs from the random forest model to estimate the importance of topographic, vegetation, geologic, and hydrologic variables in predicting EI across the 124 HUC12 sub-watersheds in our study area. Of these 124 sub-watersheds, 63 were unaffected by fire, while 61 were at least partially burned by one of the 2020 fires.

We investigated nine features with spatio-temporal coverage across our catchments of interest that represent physical influences on catchment level hydrology in western Oregon forests (Table 2). These included mean catchment burn severity (mean dNBR), geologic terrane,

Table 2
Nine metrics for random forest analysis.

Metrics	Variable type	Spatial aggregation	Description	Data source	Units	Link
Burn severity	continuous	mean	differenced normalized burn ratio	Monitoring Trends in Burn Severity (MTBS)	dNBR	https://www.mtbs.gov
Geologic Terrane	categorical	mode	age and source of geologic parent material	Oregon Department of Geology and Mineral Industries (DOGAMI)	NA	https://www.oregongeology.org/pubs/dds/p-OGDC-7.htm
Lithology	categorical	mode	description of rock type and mineralogy of parent material	Oregon Department of Geology and Mineral Industries (DOGAMI)	NA	https://www.oregongeology.org/pubs/dds/p-OGDC-7.htm
Elevation	continuous	mean	Elevation	US Geological Survey (USGS)	meters	–
Slope	continuous	mean	Slope	US Geological Survey (USGS)	degrees	–
Northing	continuous	mean	North-South component of aspect.	US Geological Survey (USGS)	ranges from 1 (north facing) to −1 (south facing)	–
Vegetation type	categorical	mode	Describes existing vegetation type on landscape	LANDFIRE	terrestrial ecological systems classification by NatureServe	https://landfire.gov/getdata.php
Succession class	categorical	mode	current vegetation condition with respect to historical successional states	LANDFIRE	NA	https://landfire.gov/getdata.php
Soil hydrologic group	categorical	mode	runoff potential of soils from NRCS	US Department of Agriculture (USDA)	NA	https://data.nal.usda.gov/dataset/united-states-general-soil-map-statsgo2

lithology, elevation, slope, north–south component of aspect (northing), soil hydrologic group, dominant existing (pre-fire) vegetation type, and succession class. We narrowed our focus to this set out of many possible features by excluding highly collinear variables for two reasons: first, correlations among features can decrease variable importance values from random forest models for both collinear variables (Debeer and Strobl, 2020; Strobl et al., 2007), and second, we only had ~ 120 catchments of study, so we limited the number of predictor variables to reduce the dimensionality of the problem. For example, we did not consider percent catchment area and mean catchment burn severity together in the model since they were highly collinear ($R^2 = 0.94$). We accounted for these variables by calculating catchment burn severity using a value of 0 for unburned pixels, thus incorporating spatial heterogeneity of burn severity and burned area in one metric.

We used the *ranger* R package to fit two random forest models—one for the 20-year pre-fire period (water years 2001–2020) and one for the post-fire period (water years 2021–2022) (Wright and Ziegler, 2017). We tuned pre-fire and post-fire model hyperparameters using k-fold cross validation to optimize model accuracy, which we measured as mean square error (MSE) on the out-of-bag dataset. Variable importance was determined using the permutation importance on the out-of-bag dataset. We sampled observations without replacement to limit bias in permutation variable importance measures (Strobl et al., 2007). After fitting, we created partial dependence plots using the *pdp* R package to visualize the direction and shape of the marginal relationships between predictor variables and modeled responses (Greenwell, 2017). We performed all our statistical analyses in R (R Core Team, 2020).

3. Results

3.1. Hydrologic response to wildfire

Our Budyko curve analysis illustrated relatively small annual deviations (Δd) of the evaporative index (EI) in the unburned, reference catchments (Table 3). For example, the mean Δd in 2021 (the first post-fire year) across all our unburned reference catchments was 0.06 ± 0.01 (SD; e.g., Fig. 3a and 3b, Figs. S2). In 2022 (the second post-fire year), the mean Δd across all our unburned reference catchments was 0.01 ± 0.01 (SD). However, we observed increasingly greater vertical deviations of EI from the fitted line of the Budyko curve in catchments with greater burned areas and burn severities (Fig. 3c to 3f, Figs. S3a to S3e). For example, in 2021 the mean Δd in catchments with < 20 % area burned was 0.10 ± 0.01 and in catchments with > 20 % area burned was 0.14 ± 0.02. Similarly, in 2022 the mean Δd in catchments with < 20 % area burned was 0.02 ± 0.01 SD and in catchments with > 20 % area burned was 0.06 ± 0.02 (SD).

Linear regression plots of the relationships between the vertical deviation from the Budyko curve (Δd) and average dNBR and area burned also illustrated a positive relationship. Statistically, there was strong evidence for a relationship between average dNBR and Δd ($F = 16.1$, $p < 0.05$, $n = 9$), with greater overall deviation and a steeper slope to the relationship in the first post-fire year (Fig. 4a). Similarly, there was strong evidence for the relationship between catchment area burned and Δd ($F = 74.2$, $p < 0.05$, $n = 9$) and also greater overall deviation and a steeper slope to the relationship in the first post-fire year (Fig. 4b). The magnitudes of Δd were lower in 2022 due to the larger precipitation amount in 2022, which led to horizontal shifts in 2022 that closed in on the fitted lines.

In addition, we assessed the impacts of wildfire disturbances on hydrology by examining relationships between changes in EI and DI. Spatial maps and box plots of the EI differences between the first post-fire year (2021) and the dry year average (Fig. 5a) showed distinct EI reductions in the burned areas. For example, while the EI difference between 2021 and dry year average in the unburned area was −0.05 ± 0.05 (SD), this difference was −0.18 ± 0.15 (SD) in the burned area. The same was observed between the second post-fire year (2022) and the wet year average (WYA) (Fig. 5b). While the EI difference between 2022 and wet year average in the unburned area was −0.03 ± 0.03 (SD), this difference was −0.10 ± 0.08 (SD) in the burned area (Fig. 6a). Besides, we compared the EI differences between post-fire years and long-term average (2001–2020) (Fig. 6b). In the unburned area, difference between 2021 and long-term average was 0.01 ± 0.05 SD, and 2022 and long-term average was −0.08 ± 0.04 (SD). In contrast, EI reductions in the burned areas were much higher than in the unburned areas in 2021 (−0.11 ± 0.13 SD) and 2022 (−0.15 ± 0.09 SD). The spatial patterns of DI in 2021 were consistent with the dry years, while the spatial patterns of DI in 2022 were consistent with the wet years (Fig. S4a). However, the spatial patterns of EI in the burned areas were not consistent with the dry and wet years (Fig. S4b), and they were derived by vegetation removal and following ET reduction. These results indicated that the EI decreases in the burned areas were substantially greater than those in the unburned areas, with the magnitude of the differences in the first post-fire year being greater than the second post-fire year.

We also compared the pre- and post-fire runoff ratio and their differences in burned and unburned catchments to investigate the impacts of different wildfire characteristics. Bar charts of the runoff ratio in the dry and wet years averages and post-fire years in the burned catchments showed an overall increase in runoff ratio during the post-fire period compared to the dry and wet years average, with larger burned areas showing higher magnitudes of increase (Fig. S5–S6). Specifically, some catchments with low burned areas showed slight decreases or no changes in runoff ratio. For example, during the first post-fire year (2021), the runoff ratio of the B1 catchment (burned area: 11.1 %) was 0.71, which was 5.3 % lower than the dry years average (0.75) during the pre-fire period. However, the runoff ratio of the B7 catchment (burned area: 94.2 %) was 1.11, which was 14.4 % higher than the dry years average (0.97). Those results were consistent with the second post-fire year (2022). The runoff ratio of the B1 catchment was 0.70, which was 9.1 % lower than the wet years average (0.77), but the runoff ratio of the B7 catchment was 1.19, which was 19.0 % higher than the wet years average (1.00).

Furthermore, runoff ratio differences (post-fire minus pre-fire) in catchments with > 20 % catchment area burned were greater than those with burned areas of < 20 % of the watershed (Fig. S5). During the first post-fire year, the average runoff ratio difference in catchments with < 20 % area burned was 0.003 ± 0.067 (SD), while the difference in catchments with > 20 % area burned was 0.062 ± 0.052 (SD). In 2022, during the second post-fire year the average runoff ratio difference in catchments with < 20 % area burned was −0.030 ± 0.040 (SD), while the difference in catchments with > 20 % area burned was 0.107 ± 0.063 (SD). In the unburned catchments, we observed slight increases or decreases in runoff ratio, except for the U4 catchment in 2022 (0.87). The average runoff ratio differences were 0.030 ± 0.032 (SD) in 2021 and 0.043 ± 0.039 (SD) in 2022 (Fig. S6). We observed overall increases

Table 3
Vertical deviations of EI from the fitted line (Δd) for the burned and unburned catchments during the post-fire period.

Catchment	Average dNBR	Burned area of the watershed (%)	Δd in 2021	Δd in 2022
B1	53.5	11.1	0.090	0.030
B2	293	23.3	0.103	0.038
B3	142.9	36.5	0.123	0.045
B4	113	36.8	0.107	0.043
B5	40.8	15.7	0.090	0.020
B6	366	79.7	0.185	0.090
B7	565.1	94.2	0.178	0.090
B8	135.9	52.8	0.130	0.052
B9	52.7	10.4	0.107	0.014
U1	0	0	0.056	0.015
U2	0	0	0.065	0.008
U3	0	0	0.050	0.004
U4	0	0	0.076	−0.003

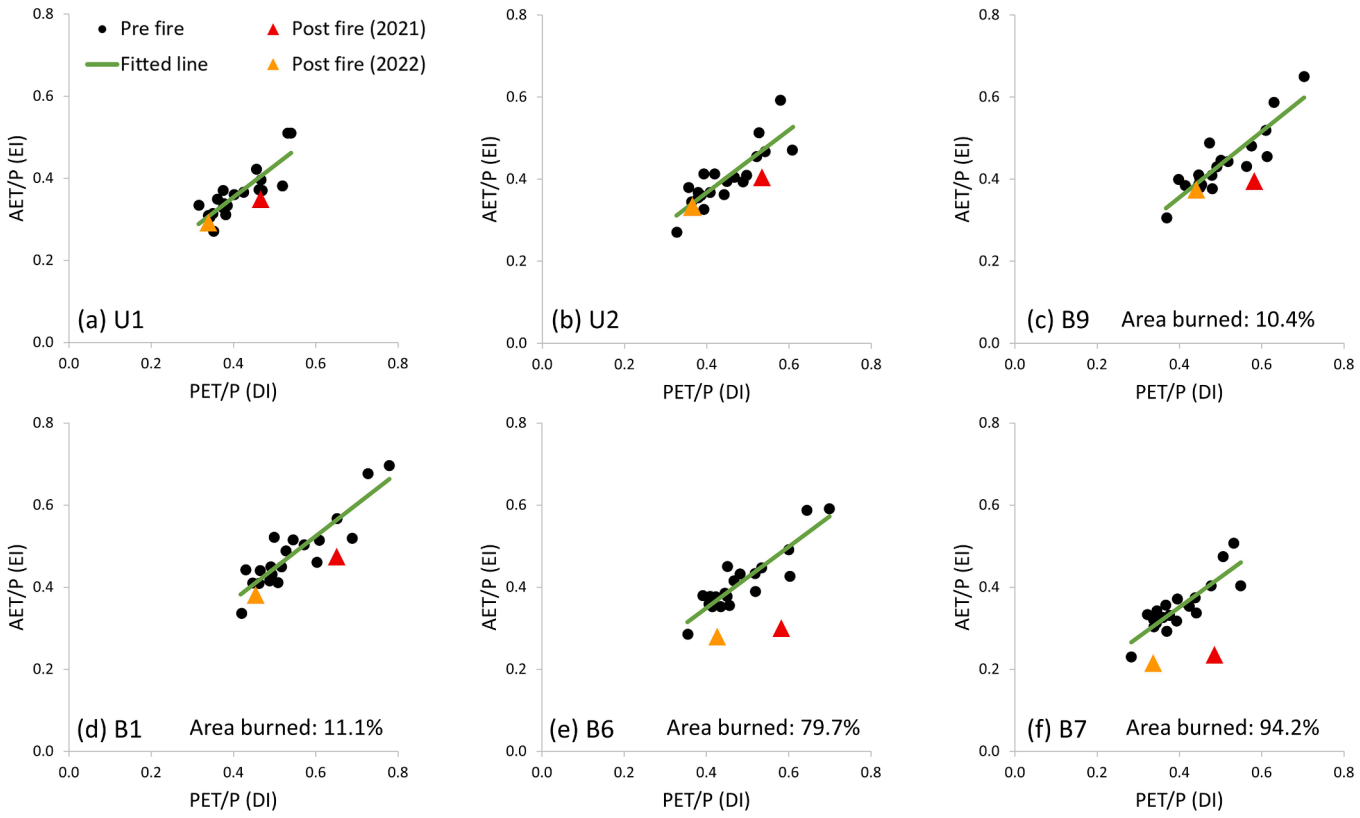

Fig. 3. Budyko curves (green line) of the evaporative index (EI) versus dryness index (DI) for representative burned and unburned catchments—the curves for the other 7 study catchments are provided in the supplemental materials. The black dots represent the pre-fire period (2001–2020), while the red and orange triangles represent the first (2021) and second (2022) post-fire years, respectively.

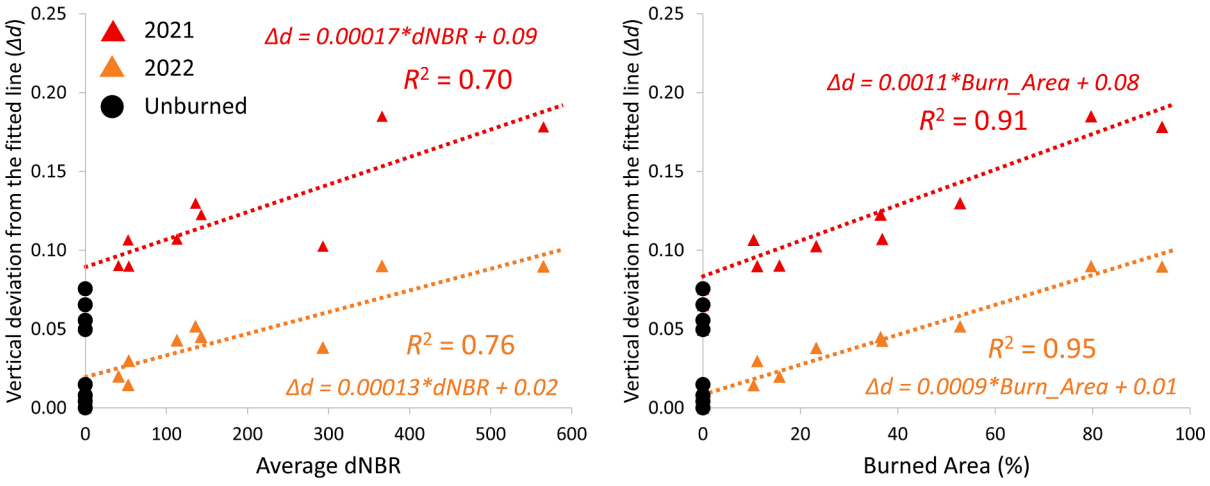

(a) Average dNBR and residual from fitted line (b) Burned area and residual from fitted line

Fig. 4. Linear regression relationships between the vertical deviation (Δd) from the Budyko curve for the nine burned and four unburned study catchments during the pre-fire years (2001–2020: black circle), first post-fire year (2021; red triangle), and second post-fire year (2022; orange triangle). The relationships for Δd are shown for (a) average dNBR and (b) percent of catchment area burned.

in runoff ratio with higher dNBR and burned area based on linear regressions between bootstrapped mean change in runoff ratio plotted against average catchment dNBR and burned area, and clear positive relationships were found between these fire characteristics and runoff ratio differences during the post-fire periods within confidence intervals of dry and wet years (Fig. 7). For example, the relationship between burned area and runoff ratio differences in 2021 ($R^2 = 0.48$, $F = 6.34$, $p < 0.05$) and 2022 ($R^2 = 0.87$, $F = 48.38$, $p < 0.05$) was stronger than those of dNBR and runoff ratio differences in 2021 ($R^2 = 0.27$, $F = 2.64$, $p = 0.15$) and 2022 ($R^2 = 0.66$, $F = 13.68$, $p < 0.05$).

During the post-fire period, higher magnitudes of EI decrease were also correlated with larger burned areas (Fig. S7–S8). For example, during the first post-fire year (2021), EI of the B5 catchment (burned area: 15.7 %) was 0.37, which was 15.9 % lower than the dry years average (0.44). Yet, EI of the B6 catchment (burned area: 79.7 %) was 0.30, which represented a 33.3 % reduction of EI compared to the dry

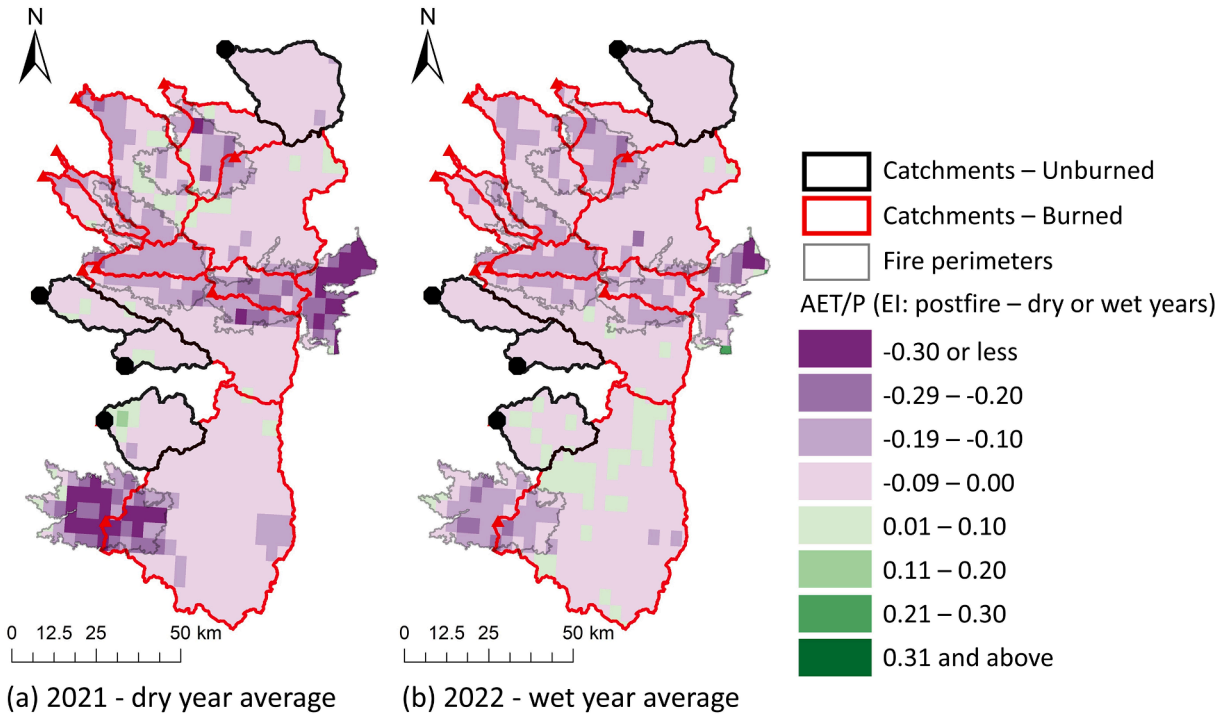

Fig. 5. Maps of the difference in evaporative index (EI) between (a) the first post-fire year (2021) and the dry year average and (b) the second post-fire year (2022) and the wet year average. Purple to light purple areas indicate decreases in EI during the post-fire period, while light green to green areas represent increases in EI.

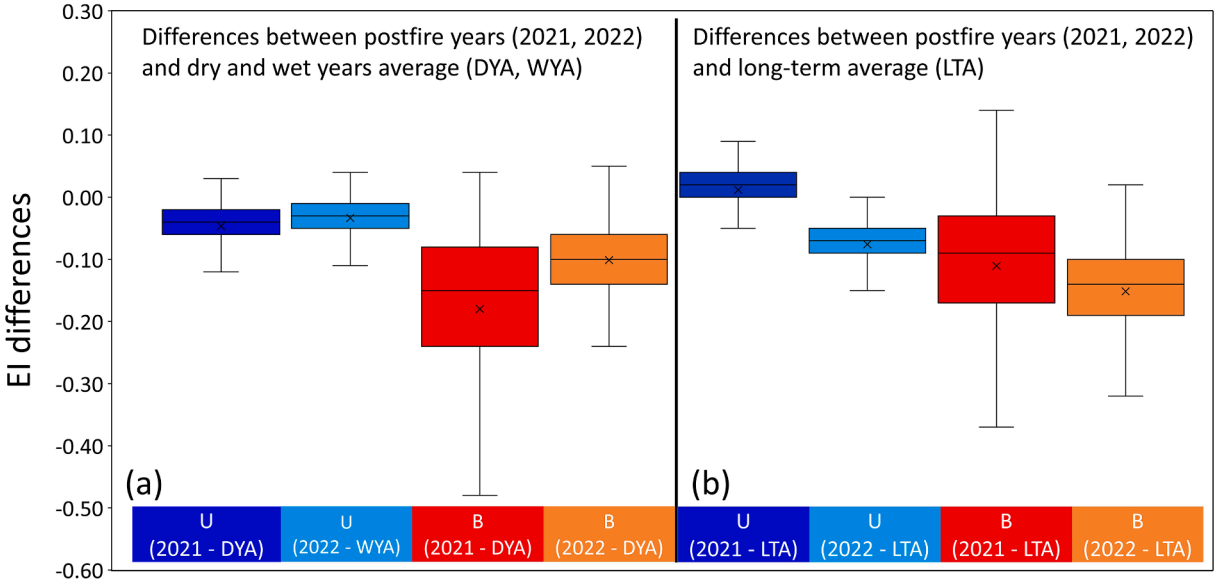

Fig. 6. Box plots for the difference in evaporative index (EI) between each of the two post-fire years (2021 and 2022) and the dry year and wet year averages, and long-term average from the pre-fire period B: Burned area, U: Unburned area, DYA: Dry years average, WYA: Wet years average, LTA: Long-term average.

years average (0.45). Similar trends were found in the second post-fire year (2022). EI of the B5 catchment during the second post-fire year was 0.32 (8.5 % reduction), while for the B6 catchment EI was 0.28 representing a reduction of 22.2 % in EI reduction.

Finally, we compared the average EI difference with < 20 % and > 20 % area burned, and larger EI differences were observed in the greater burned catchments. In 2021, the average EI difference was 0.074 ± 0.013 (SD) with < 20 % area burned, but the EI difference with > 20 % area burned was 0.101 ± 0.035 (SD). During the second post-fire year, the average EI difference with < 20 % and > 20 % area burned were 0.026 ± 0.014 (SD) and 0.060 ± 0.019 (SD), which were also consistent with the first post-fire year. In the unburned catchments, we observed minor decreases in EI compared to the average EI difference with > 20 % area burned. The average EI differences were 0.029 ± 0.015 (SD) in 2021 and 0.015 ± 0.020 (SD) in 2022. Consistently, higher decreases in EI were observed in 2021 than 2022 due to more precipitation in 2022 responsible for the horizontal shifts in DI (x-axis of the Budyko framework) (Fig. S7).

3.2. *Predictor variables of the hydrologic response to wildfire*

In the pre-fire period, elevation was the most important predictor of

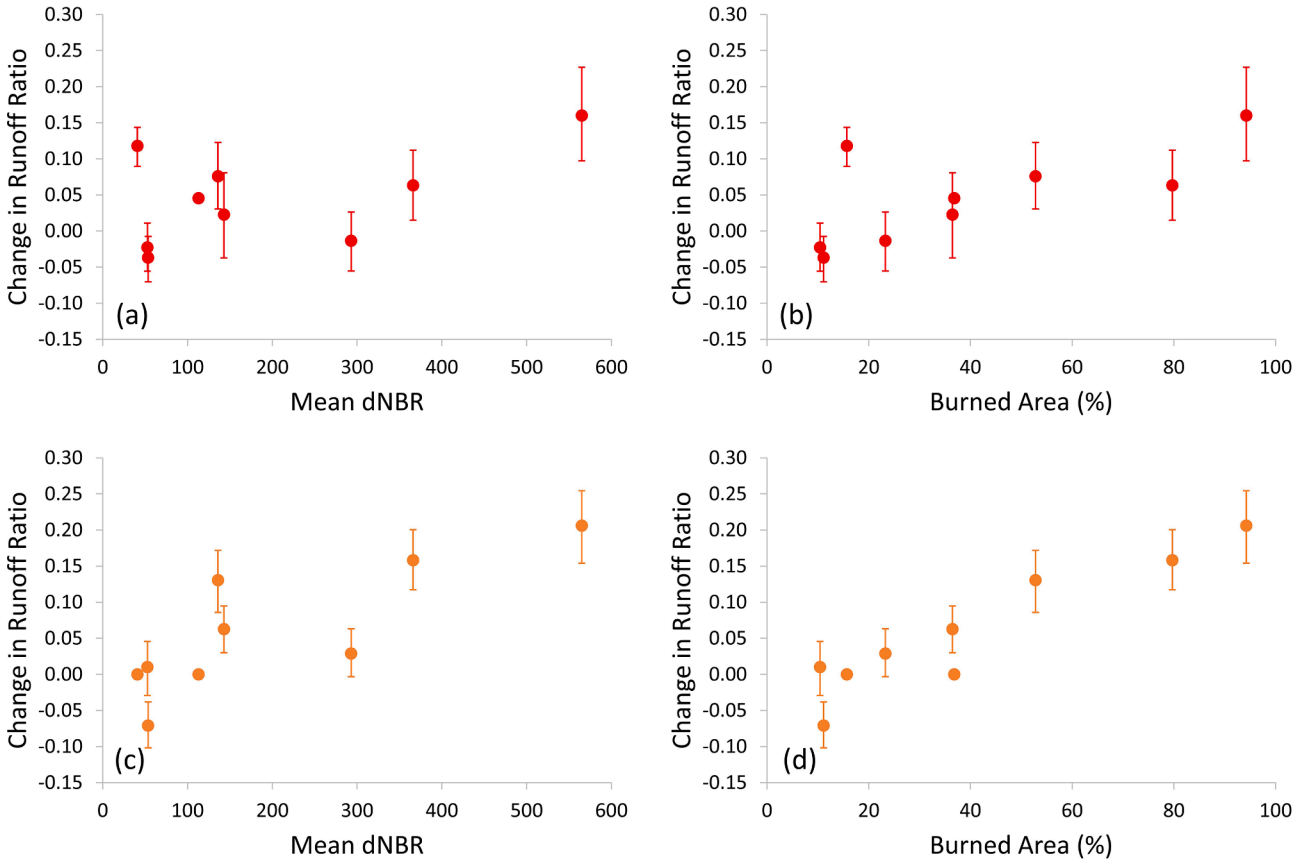

Fig. 7. Plots of the relationships between (a) bootstrapped mean change in runoff ratio during the first post-fire year (2021) and mean dNBR, (b) bootstrapped mean change in runoff ratio during the first post-fire year (2021) and percent of catchment area burned, (c) bootstrapped mean change in runoff ratio during the second post-fire year (2022) and mean dNBR, and (d) bootstrapped mean change in runoff ratio during the second post-fire year (2022) and percent of catchment area burned. The colored dots indicate bootstrapped the mean differences while the lines indicate the 95% confidence intervals.

EI, followed by slope, geologic terrane, and aspect northing. Predictors vegetation type, succession class, lithology, and soil hydrology all had relatively low predictive importance for EI during the pre-fire period (Fig. 8). In the post-fire period, burn severity was the most important predictor of EI, while elevation dropped to the third most important predictor, following slope (Fig. 8). Except for the addition of burn severity in the post-fire model, and the switching of importance between elevation and slope variables (elevation dropped to 3rd, while slope

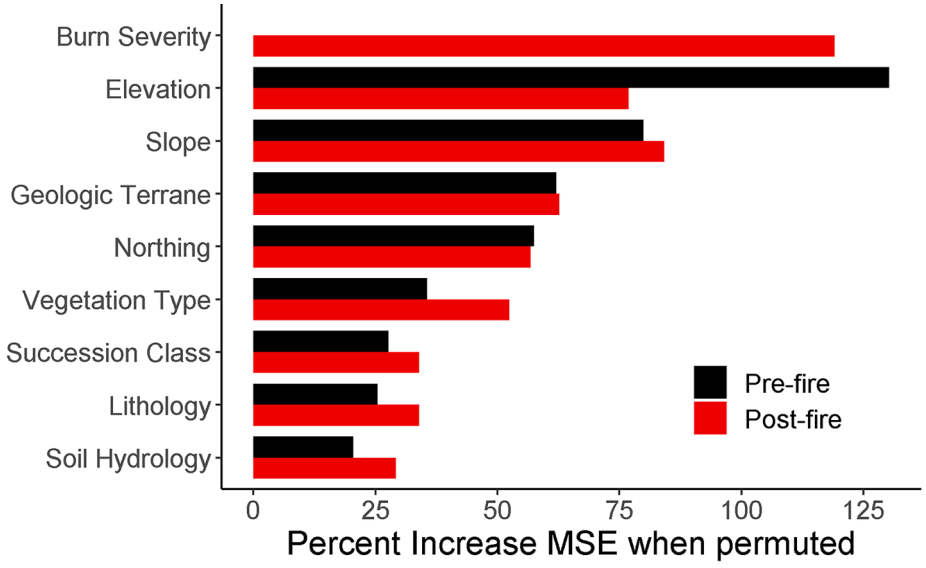

Fig. 8. Random Forest variable importance of pre- and post- fire predictor variables for predicting evaporative index (EI) in the burned and unburned watersheds. Variable importance was quantified as the percent increase in mean square error (MSE) when values of one predictor variable were randomly permuted and EI was predicted from this permuted model. Burn severity was not included in the pre-fire model.

jumped to 2nd), the remaining variables had roughly the same relative importance as the pre-fire model (Fig. 8). The random forest model for the pre-fire period explained about half of the variability (pseudo R^2 = 0.51) in EI, while the model of the post-fire period explained more variability (pseudo R^2 = 0.65), potentially due to the impact of fire on EI across the landscape. Partial dependence plots showed that EI tended to decrease as burn severity increased in our model, with the steepest decrease occurring in low to moderately burned watersheds (Fig. 9). Higher elevations were also predicted to have lower EI, but this effect was strongest at elevations above 1,500 m.

4. Discussion

In our study, we found that both burn severity and the percentage of catchment area burned were key variables for estimating runoff and ET changes in burned catchments in the Oregon Cascades. When we analyzed the Budyko curve, the most substantial reductions in the evaporative index (EI) and increases in runoff ratio occurred in catchments with high burn severity and percent area burned (>20 %). Comparatively, there was minimal or no changes in EI or the runoff ratio in catchments with less area burned (<20 %) or in catchments that were unburned. Our observations align with Hallema et al. (2018b), who observed a burned area threshold of 19 % resulted in increased streamflow in a study of 168 wildfires across the United States. Hampton and Basu (2022) also observed similar results when applying the Budyko approach to several fire events in California. Other studies have consistently shown that the severity of burns and the extent of the affected area are the most crucial factors that determine the streamflow responses. For instance, Long and Chang (2022) found that watersheds with the highest percentage of area burned experienced the largest changes in runoff coefficients in the first year after the Labor Day fires in Oregon. Similarly, Niemeyer et al. (2020) observed an increase in annual discharge across all three catchments in the Pacific Northwest in the first seven years after wildfire and post-fire forest management. Saxe et al. (2018) examined 82 burned watersheds in the western United States and found strong positive relationships between burn severity, percent area burned, and increases in runoff ratios. Furthermore, post-fire runoff ratios increased in areas burned at high severity in seven watersheds in New Mexico (Moody et al. 2008). However, the effects of wildfires on streamflow responses have been highly variable, which may be due to the complex interaction between burn characteristics, catchment physiographical characteristics, and differences in post-fire climate (Saxe et al., 2018; Long and Chang, 2023). For instance, post-fire precipitation was a critical factor in determining the post-fire hydrological response at our studied catchments. Both burned and unburned catchments exhibited horizontal shifts in the Budyko curve between 2021 and 2022, as more precipitation in 2022 influenced a decrease in DI. Compared to 2021, there was 18.7 % to 42.0 % more precipitation in 2022 in the burned and unburned catchments, and the precipitation-induced reduction in Δd in 2022 ranged from 0.060 to 0.095, which accounted for 49.7 % to 86.5 % of the $\underline{\Delta d}$ in 2021.

Despite the influence of precipitation between the two study years, the shifts in the Budyko curve and runoff ratio responses to wildfire appear to be influenced by a combination of the wildfire characteristics and catchment characteristics. The results of our random forest analysis indicated that burn severity was the most critical factor influencing changes in EI after wildfires in the western Cascades of Oregon. Specifically, mean dNBR was the strongest driver of EI across study catchments in the post-fire period. The partial dependence plot of EI vs. mean dNBR demonstrated a steep decline in EI from unburned catchments to those burned at moderate severity (Fig. 8), followed by a stabilization of EI through moderate and higher burn severities. While the negative correlation between EI and burn severity was expected (Hampton and Basu, 2022), interestingly catchments burned at high severity had a similar post-fire response in EI as catchments burned at moderate severity. The decreasing trend in EI in catchments burned at low severity was potentially linked to the post-fire decline in canopy interception and evapotranspiration (Eidenshink et al 2007). However, there may be a threshold burn severity beyond which fire did not further affect ET processes. This threshold is visible in Fig. 8 and may also be somewhat evident for runoff ratios in Fig. 7, particularly in 2022. Another possibility is that ET estimates from the SSEBop model were less accurate in highly burned areas of Pacific Northwest forests. Poon and Kinoshita (2018) observed decreased correlation between SSEBop and Ameriflux towers in burned forests in New Mexico, though they indicated the SSEBop model was accurate enough to estimate ET across their study area. Generally, the SSEBop model has been provided a reliable tool for estimating ET on a large scale; however, the accuracy of these estimates may be influenced by other factors, including land surface temperature and reference evapotranspiration values (Chen et al., 2016). SSEBop is

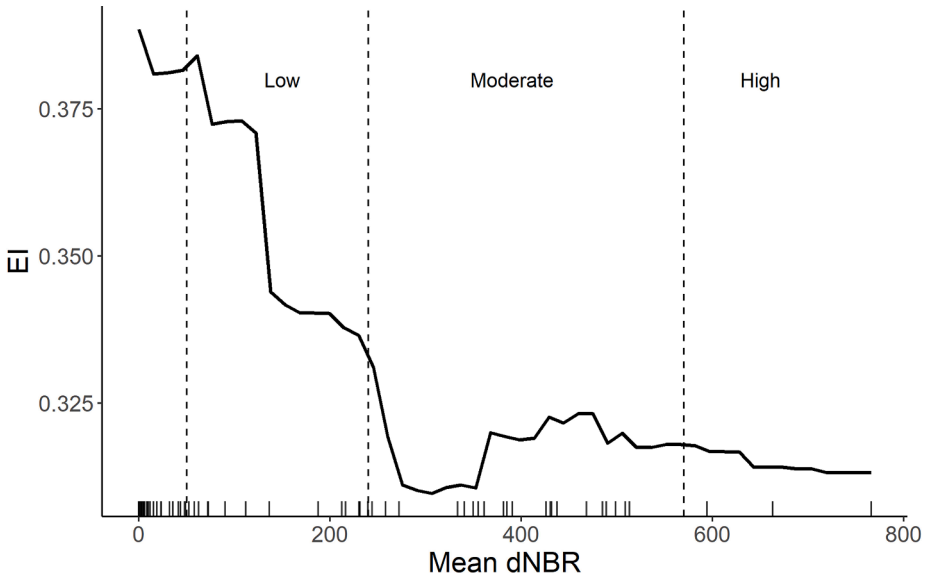

Fig. 9. Partial dependence plot showing the estimated direction and magnitude of the nonlinear relationship between mean dNBR and the evaporative index (EI) from the random forest model. Low-Moderate-High severity class breaks are from MTBS classification of dNBR data. The rug plot indicates the realized values of dNBR from our study watersheds.

particularly sensitive to land surface temperature as an input, as any pixel that has land surface temperature equal to the calibrated hot reference temperature (T_h) will have actual ET of 0 for that measurement period (McShane et al., 2017; Senay et al., 2013). This sensitivity to input could be particularly important in areas burned at moderate to high severity due to decreases in albedo and corresponding increases in remote sensed land surface temperatures and surface energy balances in burned forests (Rother and De Sales, 2021; Rother et al., 2022; Veraverbeke et al., 2012). Theoretically, high land surface temperatures after fire input into the pre-fire calibrated SSEBop model could result in predictions of 0 ET, which could explain the lower boundary on EI in the moderate and high severity burned watersheds.

In addition to fire severity, elevation and slope were also important predictors of changes in EI, followed by geologic terrain, aspect northing, vegetation type, succession class, lithology, and soil hydrology. The importance of the terrain characteristics was likely related to the strong orographic precipitation regimes in the western Cascades of Oregon, where annual precipitation varies from 1,000 to 3,000 mm across our study area (Schermerhorn, 1967). In addition, total annual precipitation and aspect may represent primary controls over the interannual variation in evapotranspiration in the western Cascades (Garcia and Tague, 2015), thus, influencing streamflow responses. Similarly, vegetation type and succession class have previously been noted as important controls over the water budget in our study region (Post and Jones, 2001).

It is not surprising that differences in geology across our study catchments influenced the runoff ratio as geology is known to exert substantial influence on groundwater transit times, catchment storage, and streamflow in our study region (Jefferson et al., 2006; Jefferson et al., 2010; Pfister et al., 2017). Furthermore, geologic influences on topography, soil type, and rock content can influence soil volumetric water content (Jarecke et al., 2021). In the Pacific Northwest, trees often rely on a combination of soil water and bedrock water storage, particularly during the summer dry season (Hahm et al., 2022). Thus, improved spatial data products on soil moisture could be advantageous to improve estimates of water availability for post-fire ET and vegetation regrowth after wildfires (Jensen et al., 2018; Thomas Ambadan et al., 2020). Indeed, due to the substantial scale of the 2020 Labor Day Fires in Oregon, there was a limited tree seedling supply from nurseries, which may have delayed recovery in some areas. Moreover, due to the high burn severity, steep slopes, and high elevation of many areas in our study region, regeneration of vegetation could be challenging, delaying the post-fire hydrologic recovery (Halofsky et al., 2020). Furthermore, hydrologic recovery can be highly variable with individual site characteristics in the Mediterranean climate (Wagenbrenner et al., 2021). Although some forests may experience relatively quick understory development, evidence from interior Pacific Northwest forests indicates that a return to pre-fire vegetation conditions could take over 50 years, with evapotranspiration (ET) requiring up to 40 years to revert to pre-fire levels (Niemeyer et al., 2020).

Our study adds to the literature by applying the Budyko framework to understand post-fire changes in EI in the Pacific Northwest, a region where it has not been applied before in a post-fire context. In addition, deriving EI from SSEBop remote sensing products (Senay et al., 2013) for un-gauged HUC12 watersheds increased the number of study watersheds and, thus, the range of catchment area burned, burn severities, and watershed characteristics across the study region. The broader range of catchment factors improved our analysis as factors such as changes in vegetation cover, plant water uptake, evapotranspiration, soil hydrophobicity, and rainfall-runoff dynamics may influence hydrologic processes in burned watersheds (Atchley et al. 2018). The nature and extent of the wildfire may also influence the hydrologic response, and studies examining the links between burn area and specific hydrologic parameters are just beginning to emerge (Havel et al. 2018; Atchley et al. 2018). Using remote sensed ET allowed improvements to our estimates of the importance of pre- and post-fire EI drivers across burned and unburned watersheds, which is crucial in determining areas that are vulnerable to post-fire effects and informing land management decisions.

It is important to acknowledge other areas of uncertainty associated with the results of our study. For instance, Senay et al. (2022) found the overestimation of ET in wet regions and underestimation in dry regions from the SSEBop model. Also, potential uncertainties may arise from the ET estimates in the western Cascades in Oregon. Even though the pre- and post-fire ET estimates from the SSEBop model were validated for the multiple wildfires in New Mexico by comparing with AmeriFlux towers (Poon and Kinoshita, 2018), the ET estimates for the 2020 Labor Days fires were not validated yet due to lack of ground observations in the burned areas. Besides, since the ET estimates from SSEBop are based on the MODIS 8-day composite 1-km resolution land surface temperature product, uncertainties in ET estimates may be related to the coarse resolution of the input temperature values from MODIS as well as its averaged temporal variability within an eight-day window. ET models based on remote sensing observations with coarse spatiotemporal resolution input data, such as SSEBop, may exhibit error propagation from the input data to the output ET estimates, which has been also observed in other models (Ferguson et al., 2010). Furthermore, it is important to consider the potential impact of dams and reservoirs in the region, which can significantly alter downstream flow patterns (Habets et al., 2018), and thus affect annualized runoff ratios. Future studies should explore how uncertainties in ET estimates after a fire event can be quantified, how the impact of reservoirs can be better understood, and how soil moisture improves the random forest model. In addition, this study only focused on the hydrologic responses of two years post-fire, and longer-term analyses that evaluate the impact of different post-fire management strategies may be necessary. Furthermore, we opted to use dNBR instead of basal area mortality or area burned to quantify fire severity, as it may be more directly linked to the process of ET in forested landscapes (Eidenshink et al., 2007). Finally, it should be noted that there may be some vegetation recovery between the first and second years of the post-fire period, which was not evaluated in this study due to differences in precipitation patterns. Other approaches should be considered to evaluate this aspect with a longer period of post-fire assessment.

5. Conclusions

In our study, we investigated the effects of wildfire on hydrologic responses in nine burned and four unburned catchments in Oregon using Budyko curve graphical technique and random forest analyses. Burn severity and percent catchment area burned were the most important factors explaining changes in streamflow and ET. Beyond burn characteristics, the hydrologic response may have been influenced by catchment characteristics and annual differences in weather. However, our analysis was also influenced by uncertainty in the spatial data products that were available to evaluate the hydrologic responses to wildfire at a regional or landscape scale. As spatial data products improve, this will improve our understanding of the complexity of hydrologic responses to wildfire. Additionally, data products reliability may be improved by pre- and post-fire validation to ensure the reliability of inputs for analyses.

In recent decades, large and high severity wildfires have increased in many parts of the world, including the Pacific Northwest of the United States. The impact of wildfires on water supply, water quality, and aquatic ecology have often been substantial and long-lasting, posing challenges for hydrologic flood prediction, drinking water treatment, and forest and ecosystem maintenance. The uncertainty in predicting response creates additional challenges for post-fire management and policy decisions. To address these challenges, it is crucial to gain a deeper understanding of how various hydrologic processes change following a forest fire and the underlying causes of those changes to improve our ability to predict post-fire hydrologic responses. Our study provided a relatively straightforward approach that relied on publicly

available data, which could provide a foundation for future analysis of post-fire effects on hydrological processes and streamflow.

Declaration of competing interest

The authors declare that they have no known competing financial interests or personal relationships that could have appeared to influence the work reported in this paper.

Acknowledgements

This work was supported by an Interagency Agreement (IA) Between US EPA, Center for Public Health and Environmental Assessment, Pacific Ecological Systems Division and the US Department of Agriculture Forest Service, Pacific Northwest Research Station (DUNS #929332484). The views expressed in this article are those of the author (s) and do not necessarily represent the views or policies of the U.S. Environmental Protection Agency.

Appendix A. Supplementary data

Supplementary data to this article can be found online at https://doi.org/10.1016/j.jhydrol.2024.131612.

References

Abatzoglou, J.T., 2013. Development of gridded surface meteorological data for ecological applications and modelling. Int. J. Climatol. 33, 121–131. https://doi.org/10.1002/joc.3413.

Abatzoglou, J.T., Kolden, C.A., Williams, A.P., Lutz, J.A., Smith, A.M.S., Abatzoglou, J.T., Kolden, C.A., Williams, A.P., Lutz, J.A., Smith, A.M.S., 2017. Climatic influences on interannual variability in regional burn severity across western US forests. Int. J. Wildland Fire 26, 269–275. https://doi.org/10.1071/WF16165.

Abatzoglou, J.T., Williams, A.P., Barbero, R., 2019. Global emergence of anthropogenic climate change in fire weather indices. Geophys. Res. Lett. 46, 326–336. https://doi.org/10.1029/2018GL080959.

Abatzoglou, J.T., Rupp, D.E., O'Neill, L.W., Sadegh, M., 2021. Compound extremes drive the western Oregon Wildfires of September 2020. Geophys. Res. Lett. 48 https://doi.org/10.1029/2021GL092520.

Abatzoglou, J.T., Williams, A.P., 2016. Impact of anthropogenic climate change on wildfire across western US forests. Proc. Natl. Acad. Sci. USA 113, 11770–11775. https://doi.org/10.1073/pnas.1607171113.

Atchley, A.L., Kinoshita, A.M., Lopez, S.R., Trader, L., Middleton, R., 2018. Simulating surface and subsurface water balance changes due to burn severity. Vadose Zone J. 17, 180099 https://doi.org/10.2136/vzj2018.05.0099.

Bart, R.R., 2016. A regional estimate of postfire streamflow change in California. Water Resour. Res. 52, 1465–1478. https://doi.org/10.1002/2014WR016553.

Beyene, M.T., Leibowitz, S.G., Pennino, M.J., 2021. Parsing weather variability and wildfire effects on the post-fire changes in daily stream flows: A quantile-based statistical approach and its application. Water Resour. Res. 57, e2020WR028029 https://doi.org/10.1029/2020WR028029.

Beyene, M.T., Leibowitz, S.G., Dunn, C.J., Bladon, K.D., 2023. To burn or not to burn: An empirical assessment of the impacts of wildfires and prescribed fires on trace element concentrations in Western US streams. Sci. Total Environ. 863, 160731 https://doi.org/10.1016/j.scitotenv.2022.160731.

Bladon, K.D., Emelko, M.B., Silins, U., Stone, M., 2014. Wildfire and the future of water supply. Environ. Sci. Technol. 48, 8936–8943. https://doi.org/10.1021/es500130g.

Blount, K., Ruybal, C.J., Franz, K.J., Hogue, T.S., 2020. Increased water yield and altered water partitioning follow wildfire in a forested catchment in the western United States. Ecohydrology 13, e2170.

Boisramé, G.F.S., Thompson, S.E., Tague (Naomi), C., Stephense, S.L., 2019. Restoring a natural fire regime alters the water balance of a Sierra Nevada catchment. Water Resour. Res. 55, 5751–5769. https://doi.org/10.1029/2018WR024098.

Breiman, L., 2001. Random Forests. Mach. Learn. 45, 5–32. https://doi.org/10.1023/A:1010933404324.

Brogan, D.J., Nelson, P.A., MacDonald, L.H., 2017. Reconstructing extreme post-wildfire floods: a comparison of convective and mesoscale events. Earth Surf. Process. Landf. 42, 2505–2522. https://doi.org/10.1002/esp.4194.

Budyko, M.I., 1961. The heat balance of the Earth's surface. Sov. Geogr. 2, 3–13. https://doi.org/10.1080/00385417.1961.10770761.

Budyko, M.I., 1974. Climate and life. Press, Acad, p. 508.

Burke, M., Driscoll, A., Heft-Neal, S., Xue, J., Burney, J., Wara, M., 2021. The changing risk and burden of wildfire in the United States. Proc. Natl. Acad. Sci. USA 118. https://doi.org/10.1073/pnas.2011048118.

Busing, R.T., 2004. A forest vegetation database for Western Oregon. U.S. Geological Survey. Open File Report 2004-1249. p. 15. https://doi.org/10.3133/ofr20041249.

Chen, J., McGuire, K.J., Stewart, R.D., 2020. Effect of soil water-repellent layer depth on post-wildfire hydrological processes. Hydrol. Process. 34, 270–283. https://doi.org/10.1002/hyp.13583.

Chen, M., Senay, G.B., Singh, R.K., Verdin, J.P., 2016. Uncertainty analysis of the Operational Simplified Surface Energy Balance (SSEBop) model at multiple flux tower sites. J. Hydrol. 536, 384–399. https://doi.org/10.1016/j.jhydrol.2016.02.026.

Collar, N.M., Saxe, S., Rust, A.J., Hogue, T.S., 2021. A CONUS-scale study of wildfire and evapotranspiration: Spatial and temporal response and controlling factors. J. Hydrol. 603, 127162 https://doi.org/10.1016/j.jhydrol.2021.127162.

Costanza, R., d'Arge, R., de Groot, R., Farber, S., Grasso, M., Hannon, B., Limburg, K., Naeem, S., O'Neill, R.V., Paruelo, J., Raskin, R.G., Sutton, P., van den Belt, M., 1997. The value of the world's ecosystem services and natural capital. Nature 387, 253–260. https://doi.org/10.1038/387253a0.

Debeer, D., Strobl, C., 2020. Conditional permutation importance revisited. BMC Bioinformatics 21, 307. https://doi.org/10.1186/s12859-020-03622-2.

Dudley, N., Stolton, S., 2003. Running pure: The importance of forest protected areas to drinking water. World Bank/WWF Alliance for Forest Conservation and Sustainable Use.

Ebel, B.A., Moody, J.A., Martin, D.A., 2012. Hydrologic conditions controlling runoff generation immediately after wildfire. Water Resour. Res. 48 https://doi.org/10.1029/2011WR011470.

Eidenshink, J., Schwind, B., Brewer, K., Zhu, Z.L., Quayle, B., Howard, S., 2007. A project for monitoring trends in burn severity. Fire Ecology 3, 3–21. https://doi.org/10.4996/fireecology.0301003.

Emelko, M.B., Silins, U., Bladon, K.D., Stone, M., 2011. Implications of land disturbance on drinking water treatability in a changing climate: Demonstrating the need for "source water supply and protection" strategies. Water Res. 45, 461–472. https://doi.org/10.1016/j.watres.2010.08.051.

Emelko, M.B., Stone, M., Silins, U., Allin, D., Collins, A.L., Williams, C.H.S., Martens, A. M., Bladon, K.D., 2016. Sediment-phosphorus dynamics can shift aquatic ecology and cause downstream legacy effects after wildfire in large river systems. Glob. Change Biol. 22, 1168–1184. https://doi.org/10.1111/gcb.13073.

Ferguson, C.R., Sheffield, J., Wood, E.F., Gao, H., 2010. Quantifying uncertainty in a remote sensing-based estimate of evapotranspiration over continental USA. Int. J. Remote Sens. 31, 3821–3865. https://doi.org/10.1080/01431161.2010.483490.

Garcia, E.S., Tague, C.L., 2015. Subsurface storage capacity influences climate–evapotranspiration interactions in three western United States catchments. Hydrol. Earth Syst. Sci. 19, 4845–4858. https://doi.org/10.5194/hess-19-4845-2015.

Greenwell, B.M., 2017. pdp: An R Package for Constructing Partial Dependence Plots. R J. 9, 421–436.

Guo, Y., Zhang, L., Zhang, Y., Wang, Z., Zheng, H.X., 2021. Estimating impacts of wildfire and climate variability on streamflow in Victoria. Australia. Hydrol. Process. 35, e14439.

Habets, F., Molénat, J., Carluer, N., Douez, O., Leenhardt, D., 2018. The cumulative impacts of small reservoirs on hydrology: A review. Sci. Total Environ. 643, 850–867. https://doi.org/10.1016/j.scitotenv.2018.06.188.

Hahm, W.J., Dralle, D.N., Sanders, M., Bryk, A.B., Fauria, K.E., Huang, M.H., Hudson-Rasmussen, B., Nelson, M.D., Pedrazas, M.A., Schmidt, L., Whiting, J., 2022. Bedrock vadose zone storage dynamics under extreme drought: consequences for plant water availability, recharge, and runoff. Water Resour. Res. 58 https://doi.org/10.1029/2021WR031781.

Hallema, D.W., Robinne, F.-N., Bladon, K.D., 2018a. Reframing the challenge of global wildfire threats to water supplies. Earths Future 6, 772–776. https://doi.org/10.1029/2018EF000867.

Hallema, D.W., Sun, G., Caldwell, P.V., Norman, S.P., Cohen, E.C., Liu, Y., Bladon, K.D., McNulty, S.G., 2018b. Burned forests impact water supplies. Nat. Commun. 9, 1307. https://doi.org/10.1038/s41467-018-03735-6.

Halofsky, J.E., Peterson, D.L., Harvey, B.J., 2020. Changing wildfire, changing forests: the effects of climate change on fire regimes and vegetation in the Pacific Northwest, USA. Fire Ecol. 16, 1–26. https://doi.org/10.1186/s42408-019-0062-8.

Hampton, T.B., Basu, N.B., 2022. A novel Budyko-based approach to quantify post-forest-fire streamflow response and recovery timescales. J. Hydrol. 608, 127685 https://doi.org/10.1016/j.jhydrol.2022.127685.

Havel, A., Tasdighi, A., Arabi, M., 2018. Assessing the hydrologic response to wildfires in mountainous regions. Hydrol. Earth Syst. Sci. 22, 2527–2550. https://doi.org/10.5194/hess-22-2527-2018.

Higuera, P.E., Abatzoglou, J.T., 2021. Record-setting climate enabled the extraordinary 2020 fire season in the western United States. Glob. Change Biol. 27, 1–2. https://doi.org/10.1111/gcb.15388.

Hohner, A.K., Rhoades, C.C., Wilkerson, P., Rosario-Ortiz, F.L., 2019. Wildfires alter forest watersheds and threaten drinking water quality. Acc. Chem. Res. 52, 1234–1244. https://doi.org/10.1021/acs.accounts.8b00670.

Holden, Z.A., Swanson, A., Luce, C.H., Jolly, W.M., Maneta, M., Oyler, J.W., Warren, D. A., Parsons, R., Affleck, D., 2018. Decreasing fire season precipitation increased recent western US forest wildfire activity. Proc. Natl. Acad. Sci. USA 115, E8349–E8357. https://doi.org/10.1073/pnas.1802316115.

Jaramillo, F., Cory, N., Arheimer, B., Laudon, H., van der Velde, Y., Hasper, T.B., Teutschbein, C., Uddling, J., 2018. Dominant effect of increasing forest biomass on evapotranspiration: interpretations of movement in Budyko space. Hydrol. Earth Syst. Sci. 22, 567–580. https://doi.org/10.5194/hess-22-567-2018.

Jarecke, K.M., Bladon, K.D., Wondzell, S.M., 2021. The influence of local and nonlocal factors on soil water content in a steep forested catchment. Water Resour. Res. 57, e2020WR028343 https://doi.org/10.1029/2020WR028343.

Jefferson, A., Grant, G.E., Lewis, S.L., Lancaster, S.T., 2010. Coevolution of hydrology and topography on a basalt landscape in the Oregon Cascade Range, USA. Earth Surf. Process. Landf. 35, 803–816. https://doi.org/10.1002/esp.1976.
Jefferson, A., Grant, G., Rose, T., 2006. Influence of volcanic history on groundwater patterns on the west slope of the Oregon High Cascades. Water Resour. Res. 42, W12411. https://doi.org/10.1029/2005WR004812.
Jensen, D., Reager, J.T., Zajic, B., Rousseau, N., Rodell, M., Hinkley, E., 2018. The sensitivity of US wildfire occurrence to pre-season soil moisture conditions across ecosystems. Environ. Res. Lett. 13, 014021 https://doi.org/10.1088/1748-9326/aa9853.
Jolly, W.M., Cochrane, M.A., Freeborn, P.H., Holden, Z.A., Brown, T.J., Williamson, G.J., Bowman, D.M.J.S., 2015. Climate-induced variations in global wildfire danger from 1979 to 2013. Nat. Commun. 6, 7537. https://doi.org/10.1038/ncomms8537.
Jones, J.A., Achterman, G.L., Augustine, L.A., Creed, I.F., Ffolliott, P.F., MacDonald, L., Wemple, B.C., 2009. Hydrologic effects of a changing forested landscape-challenges for the hydrological sciences. Hydrol. Process. 23, 2699–2704. https://doi.org/10.1002/hyp.7404.
Key, C.H., Benson, N.C., 2006. Landscape Assessment: Ground measure of severity, the composite burn index; and remote sensing of severity, the normalized burn ratio. (FIREMON: Fire Effects Monitoring and Inventory System.). USDA Forest Service, Rocky Mountain Research Station, Ogden, UT.
Kinoshita, A.M., Hogue, T.S., 2015. Increased dry season water yield in burned watersheds in Southern California. Environ. Res. Lett. 10, 014003 https://doi.org/10.1088/1748-9326/10/1/014003.
Kottek, M., Grieser, J., Beck, C., Rudolf, B., Rubel, F., 2006. World Map of the Köppen-Geiger climate classification updated. Meteorol. z. 15, 259–263. https://doi.org/10.1127/0941-2948/2006/0130.
Lavabre, J., Torres, D.S., Cernesson, F., 1993. Changes in the hydrological response of a small Mediterranean basin a year after a wildfire. J. Hydrol. 142, 273–299. https://doi.org/10.1016/0022-1694(93)90014-Z.
Lee, S., 2020. Impact of wildfire on annual water yield in large watersheds. Department of Civil Engineering, University of Idaho, Ph.D. Dissertation, p. 97.
Li, C., Wang, L., Wanrui, W., Qi, J., Linshan, Y., Zhang, Y., Lei, W., Cui, X., Wang, P., 2018. An analytical approach to separate climate and human contributions to basin streamflow variability. J. Hydrol. 559, 30–42. https://doi.org/10.1016/j.jhydrol.2018.02.019.
Long, W.B., Chang, H., 2022. Event scale analysis of streamflow response to wildfire in Oregon, 2020. Hydrology 9, 157. https://doi.org/10.3390/hydrology9090157.
Long, W.B., Chang, H., 2023. Spatial analysis of streamflow trends in burned watersheds across the western contiguous United States. Hydrol. Process. 37, e14949 https://doi.org/10.1002/hyp.14949.
Ma, Q., Bales, R.C., Rungee, J., Conklin, M.H., Collins, B.M., Goulden, M.L., 2020. Wildfire controls on evapotranspiration in California's Sierra Nevada. J. Hydrol. 590, 125364 https://doi.org/10.1016/j.jhydrol.2020.125364.
Madin, I.P., 2009. Oregon: A Geologic History, Oregon Department of Geology and Mineral Industries Interpretive Series Map 28. [WWW Document]. URL https://www.oregongeology.org/pubs/ims/p-ims-028.htm (accessed 6.26.23).
Mahat, V., Silins, U., Anderson, A., 2016. Effects of wildfire on the catchment hydrology in southwest Alberta. Catena 147, 51–60. https://doi.org/10.1016/j.catena.2016.06.040.
McShane, R.R., Driscoll, K.P., Sando, R., 2017. A review of surface energy balance models for estimating actual evapotranspiration with remote sensing at high spatiotemporal resolution over large extents. Sci. Inves. Rep. 2017–5087 https://doi.org/10.3133/sir20175087.
Moody, J.A., Ebel, B.A., 2014. Infiltration and runoff generation processes in fire-affected soils. Hydrol. Process. 28, 3432–3453. https://doi.org/10.1002/hyp.9857.
Moody, J.A., Martin, D.A., Haire, S.L., Kinner, D.A., 2008. Linking runoff response to burn severity after a wildfire. Hydrol. Process. 22, 2063–2074. https://doi.org/10.1002/hyp.6806.
Moody, J.A., Shakesby, R.A., Robichaud, P.R., Cannon, S.H., Martin, D.A., 2013. Current research issues related to post-wildfire runoff and erosion processes. Earth-Sci. Rev. 122, 10–37. https://doi.org/10.1016/j.earscirev.2013.03.004.
Moody, J.A., Ebel, B.A., Nyman, P., Martin, D.A., Stoof, C.R., McKinley, R., 2015. Relations between soil hydraulic properties and burn severity. Int. J. Wildland 25, 279–293. https://doi.org/10.1071/WF14062.
Neary, D., 2011. Impacts of wildfire severity on hydraulic conductivity in forest, woodland, and grassland soils. In: Elango, L. (Ed.), Hydraulic Conductivity - Issues, Determination and Applications. InTech, New York, NY, pp. 123–142. https://doi.org/10.5772/20872.
Niemeyer, R.J., Bladon, K.D., Woodsmith, R.D., 2020. Long-term hydrologic recovery after wildfire and post-fire forest management in the interior Pacific Northwest. Hydrol. Process. 34, 1182–1197. https://doi.org/10.1002/hyp.13665.
Noske, P.J., Nyman, P., Lane, P.N.J., Sheridan, G.J., 2016. Effects of aridity in controlling the magnitude of runoff and erosion after wildfire. Water Resour. Res. 52, 4338–4357. https://doi.org/10.1002/2015WR017611.
Pfister, L., Martínez-Carreras, N., Hissler, C., Klaus, J., Carrer, G.E., Stewart, M.K., McDonnell, J.J., 2017. Bedrock geology controls on catchment storage, mixing, and release: A comparative analysis of 16 nested catchments. Hydrol. Process. 31, 1828–1845. https://doi.org/10.1002/hyp.11134.
Poon, P.K., Kinoshita, A.M., 2018. Spatial and temporal evapotranspiration trends after wildfire in semi-arid landscapes. J. Hydrol. 559, 71–83. https://doi.org/10.1016/j.jhydrol.2018.02.023.
Post, D.A., Jones, J.A., 2001. Hydrologic regimes of forested, mountainous, headwater basins in New Hampshire, North Carolina, Oregon, and Puerto Rico. Adv. Water Resour. 24, 1195–1210. https://doi.org/10.1016/S0309-1708(01)00036-7.
PRISM Climate Group, 2022. PRISM 30 years precipitation data (4km).
R Core Team, 2020. R: A language and environment for statistical computing.
Rasmussen, M., Lord, R., Fay, R., Baribault, T., Goodnow, R., 2021. 2020 Labor Day Fires: Economic impacts. Oregon Forest Resources Institute.
Reaver, N.G., Kaplan, D.A., Klammler, H., Jawitz, J.W., 2022. Theoretical and empirical evidence against the Budyko catchment trajectory conjecture. Hyd. Earth Sys. Sci. 26, 1507–1525. https://doi.org/10.5194/hess-26-1507-2022.
Rhoades, C.C., Entwistle, D., Butler, D., Rhoades, C.C., Entwistle, D., Butler, D., 2011. The influence of wildfire extent and severity on streamwater chemistry, sediment and temperature following the Hayman Fire. ColoradoA. Int. J. Wildland Fire 20, 430–442. https://doi.org/10.1071/WF09086.
Rhoades, C.C., Chow, A.T., Covino, T.P., Fegel, T.S., Pierson, D.N., Rhea, A.E., 2019. The legacy of a severe wildfire on stream nitrogen and carbon in headwater catchments. Ecosystems 22, 643–657. https://doi.org/10.1007/s10021-018-0293-6.
Robinne, F.-N., Hallema, D.W., Bladon, K.D., Buttle, J.M., 2020. Wildfire impacts on hydrologic ecosystem services in North American high-latitude forests: A scoping review. J. Hydrol. 581, 124360 https://doi.org/10.1016/j.jhydrol.2019.124360.
Rother, D., De Sales, F., 2021. Impact of wildfire on the surface energy balance in six California case studies. Boundary-Layer Meteo. 178, 143–166. https://doi.org/10.1007/s10546-020-00562-5.
Rother, D.E., De Sales, F., Stow, D., McFadden, J., 2022. Impacts of burn severity on short-term postfire vegetation recovery, surface albedo, and land surface temperature in California ecoregions. Plos One 17, e0274428. https://doi.org/10.1371/journal.pone.0274428.
Rust, A.J., Hogue, T.S., Saxe, S., McCray, J., Rust, A.J., Hogue, T.S., Saxe, S., McCray, J., 2018. Post-fire water-quality response in the western United States. Int. J. Wildland Fire 27, 203–216. https://doi.org/10.1071/WF17115.
Saxe, S., Hogue, T.S., Hay, L., 2018. Characterization and evaluation of controls on post-fire streamflow response across western US watersheds. Hydrol. Earth Syst. Sci. 22, 1221–1237. https://doi.org/10.5194/hess-22-1221-2018.
Schermerhorn, V.P., 1967. Relations between topography and annual precipitation in western Oregon and Washington. Water Resour. Res. 3, 707–711. https://doi.org/10.1029/WR003i003p00707.
Senay, G.B., Bohms, S., Singh, R.K., Gowda, P.H., Velpuri, N.M., Alemu, H., Verdin, J.P., 2013. Operational evapotranspiration mapping using remote sensing and weather datasets: A new parameterization for the SSEB approach. JAWRA J. Am. Water Resour. Assoc. 49, 577–591. https://doi.org/10.1111/jawr.12057.
Senay, G.B., Friedrichs, M., Morton, C., Parrish, G.E., Schauer, M., Khand, K., Kagone, S., Boiko, O., Huntington, J., 2022. Mapping actual evapotranspiration using Landsat for the conterminous United States: Google Earth Engine implementation and assessment of the SSEBop model. Rem. Sen. Environ. 275, 113011 https://doi.org/10.1016/j.rse.2022.113011.
Shuman, J.K., Balch, J.K., Barnes, R.T., Higuera, P.E., Roos, C.I., Schwilk, D.W., Stavros, E.N., Banerjee, T., Bela, M.M., Bendix, J., Bertolino, S., Bililign, S., Bladon, K.D., Brando, P., Breidenthal, R.E., Buma, B., Calhoun, D., Carvalho, L.M.V., Cattau, M.E., Cawley, K.M., Chandra, S., Chipman, M.L., Cobian-Iñiguez, J., Conlisk, E., Coop, J.D., Cullen, A., Davis, K.T., Dayalu, A., De Sales, F., Dolman, M., Ellsworth, L.M., Franklin, S., Guiterman, C.H., Hamilton, M., Hanan, E.J., Hansen, W.D., Hantson, S., Harvey, B.J., Holz, A., Huang, T., Hurteau, M.D., Ilangakoon, N.T., Jennings, M., Jones, C., Klimaszewski-Patterson, A., Kobziar, L.N., Kominoski, J., Kosovic, B., Krawchuk, M.A., Laris, P., Leonard, J., Loria-Salazar, S. M., Lucash, M., Mahmoud, H., Margolis, E., Maxwell, T., McCarty, J.L., McWethy, D. B., Meyer, R.S., Miesel, J.R., Moser, W.K., Nagy, R.C., Niyogi, D., Palmer, H.M., Pellegrini, A., Poulter, B., Robertson, K., Rocha, A.V., Sadegh, M., Santos, F., Scordo, F., Sexton, J.O., Sharma, A.S., Smith, A.M.S., Soja, A.J., Still, C., Swetnam, T., Syphard, A.D., Tingley, M.W., Tohidi, A., Trugman, A.T., Turetsky, M., Varner, J.M., Wang, Y., Whitman, T., Yelenik, S., Zhang, X., 2022. Reimagine fire science for the anthropocene. PNAS Nexus 1, pgac115. https://doi.org/10.1093/pnasnexus/pgac115.
Strobl, C., Boulesteix, A.-L., Zeileis, A., Hothorn, T., 2007. Bias in random forest variable importance measures: Illustrations, sources and a solution. BMC Bioinformatics 8, 25. https://doi.org/10.1186/1471-2105-8-25.
Thomas Ambadan, J., Oja, M., Gedalof, Z., Berg, A.A., 2020. Satellite-observed soil moisture as an indicator of wildfire risk. Remote Sens. 12, 1543. https://doi.org/10.3390/rs12101543.
van der Werf, G.R., Randerson, J.T., Giglio, L., Collatz, G.J., Kasibhatla, P.S., Arellano, A. F.J., 2006. Interannual variability in global biomass burning emissions from 1997 to 2004. Atmospheric Chem. Phys. 6, 3423–3441. https://doi.org/10.5194/acp-6-3423-2006.
Veraverbeke, S., Verstraeten, W.W., Lhermitte, S., Van De Kerchove, R., Goossens, R., 2012. Assessment of post-fire changes in land surface temperature and surface albedo, and their relation with fire–burn severity using multitemporal MODIS imagery. Inter. J. Wildland Fire 21, 243–256. https://doi.org/10.1071/WF10075.
Vieira, D.C.S., Malvar, M.C., Martins, M.A.S., Serpa, D., Keizer, J.J., 2018. Key factors controlling the post-fire hydrological and erosive response at micro-plot scale in a recently burned Mediterranean forest. Geomorphology 319, 161–173. https://doi.org/10.1016/j.geomorph.2018.07.014.
Wagenbrenner, J.W., Ebel, B.A., Bladon, K.D., Kinoshita, A.M., 2021. Post-wildfire hydrologic recovery in Mediterranean climates: A systematic review and case study to identify current knowledge and opportunities. J. Hydrol. 602, 126772 https://doi.org/10.1016/j.jhydrol.2021.126772.
Wampler, K.A., Bladon, K.D., Faramarzi, M., 2023. Modeling wildfire effects on streamflow in the Cascade Mountains, Oregon, USA. J. Hydrol. 621, 129585 https://doi.org/10.1016/j.jhydrol.2023.129585.
Wang, D., Hejazi, M., 2011. Quantifying the relative contribution of the climate and direct human impacts on mean annual streamflow in the contiguous United States. Water Resour. Res. 47, W00J12. https://doi.org/10.1029/2010WR010283.

Wang, H., Stephenson, S.R., 2018. Quantifying the impacts of climate change and land use/cover change on runoff in the lower Connecticut River Basin. Hydrol. Process. 32, 1301–1312. https://doi.org/10.1002/hyp.11509.

Wang, J., Stern, M.A., King, V.M., Alpers, C.N., Quinn, N.W.T., Flint, A.L., Flint, L.E., 2020. PFHydro: A new watershed-scale model for post-fire runoff simulation. Environ. Model. Softw. 123, 104555 https://doi.org/10.1016/j.envsoft.2019.104555.

Warren, D.R., Roon, D.A., Swartz, A.G., Bladon, K.D., 2022. Loss of riparian forests from wildfire led to increased stream temperatures in summer, yet salmonid fish persisted. Ecosphere 13, e4233. https://doi.org/10.1002/ecs2.4233.

Westerling, A.L., 2016. Increasing western US forest wildfire activity: sensitivity to changes in the timing of spring. Philos. Trans. r. Soc. B Biol. Sci. 371, 20150178. https://doi.org/10.1098/rstb.2015.0178.

Williams, A.P., Livneh, B., McKinnon, K.A., Hansen, W.D., Mankin, J.S., Cook, B.I., Smerdon, J.E., Varuolo-Clarke, A.M., Bjarke, N.R., Juang, C.S., Lettenmaier, D.P., 2022. Growing impact of wildfire on western US water supply. Proc. Natl. Acad. Sci. 119, e2114069119 https://doi.org/10.1073/pnas.2114069119.

Wine, M.L., Cadol, D., 2016. Hydrologic effects of large southwestern USA wildfires significantly increase regional water supply: fact or fiction? Environ. Res. Lett. 11, 085006 https://doi.org/10.1088/1748-9326/11/8/085006.

Wright, M.N., Ziegler, A., 2017. ranger: A fast implementation of random forests for high dimensional data in C++ and R. J. Stat. Softw. 77, 1–17. https://doi.org/10.18637/jss.v077.i01.

Zema, D.A., 2021. Postfire management impacts on soil hydrology. Curr. Opin. Environ. Sci. Health 21, 100252. https://doi.org/10.1016/j.coesh.2021.100252.

Zituni, R., Wittenberg, L., Malkinson, D., 2019. The effects of post-fire forest management on soil erosion rates 3 and 4 years after a wildfire, demonstrated on the 2010 Mount Carmel fire. Int. J. Wildland Fire 28, 377. https://doi.org/10.1071/WF18116.